ACS Sustainable Chemistry & Engineering

Research Article

pubs.acs.org/journal/ascecg

Role of PEG Segment in Stereocomplex Crystallization for PLLA/PDLA-*b*-PEG-*b*-PDLA Blends

Yan Song,[†,§] Dujin Wang,[†] Ni Jiang,*[,†] and Zhihua Gan*[,‡]

[†]CAS Key Laboratory of Engineering Plastics, Institute of Chemistry, Chinese Academy of Sciences (CAS), Beijing 100190, China

[‡]State Key Laboratory of Organic−Inorganic Composites, Beijing Laboratory of Biomedical Materials, College of Life Sciences and Technology, Beijing University of Chemical Technology, Beijing 100029, China

[§]University of Chinese Academy of Sciences, Beijing 100049, China

Supporting Information

ABSTRACT: The isothermal crystallization behavior and morphology of neat poly(L-lactic acid) (PLLA) and its blends with poly(D-lactic acid) (PDLA) and PDLA-*b*-poly(ethylene glycol) (PEG)-*b*-PDLA have been investigated. The glass transition temperature of the PLLA/PDLA blend, and especially the PLLA/PDLA-*b*-PEG-*b*-PDLA blend, is much lower than that of neat PLLA, indicating the plasticization effect of both low molecular weight PDLA and flexible PEG block. Both the PLLA/PDLA and PLLA/PDLA-*b*-PEG-*b*-PDLA blends can form stereocomplex (SC) crystals. However, the PDLA in the PLLA/PDLA blend postponed the crystallization rate of the blend, whereas the PEG chains in PLLA/PDLA-*b*-PEG-*b*-PDLA not only promoted the formation of SC crystals but also facilitated the crystallization of the PLLA matrix. The evolution of the crystal structure and morphologies of PLLA and its blends during the isothermal crystallization process have revealed the significant role of flexible PEG chains in the stereocomplex crystallization.

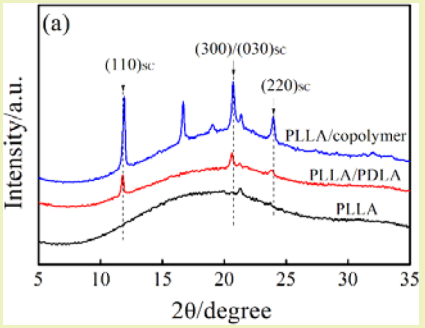

KEYWORDS: *Poly(L-lactic acid), PDLA-b-PEG-b-PDLA, Blend, Stereocomplex crystallization, Morphology*

INTRODUCTION

Biobased materials have shown great potential to replace gradually oil-based polymers in terms of sustainability and eco-friendly properties. Poly(lactic acid) (PLA) derived from renewable sources has obtained extensive attention in the fields of biomedicine and environmental protection due to its good biocompatibility and biodegradability.[1] PLA can be produced by either condensation polymerization or ring-opening polymerization from natural lactic acid or its derivative lactide. However, the slow crystallization rate, brittleness and poor thermal stability of PLA prohibit its widespread application. Therefore, great efforts to improve the impact strength and thermal stability of PLA have been performed in recent years by modifying the crystallization rate and morphology.[2,3] Among them, the physical blending method, which only involves the physical interaction without complicated chemical techniques, has been primarily considered.

As a biocompatible and flexible polymer, polyethylene glycol (PEG) is a good candidate for modifying the toughness of PLA via physical blending.[4] PEG chains are flexible and can act as a diluting agent in a PLA/PEG blend to reduce the interaction among PLA chains. Consequently, the toughness of PLA is improved after blending with less than 50 wt % PEG.[5] The glass transition temperature (T_g) of PLA is decreased by adding PEG with lower molecular weight and higher content.[6,7] Moreover, the crystallization of PLA is also severely reduced with high content of PEG.[8] In addition, the miscibility and crystallization behavior of PLA/PEG blends are also influenced by the molecular weight,[6] end group[9] and content[5] of PEG. However, due to the water-solubility of PEG, or the phase separation during the aging process, the PLA/PEG blend cannot maintain the modified mechanical property over time.[8,10,11] Thus, it is worth studying how to modify the structure of PEG for effectively utilizing the advantages of PEG to improve the properties of PLA via blending.

It is known that lactic acid has three types of isomers, i.e., L-lactic acid (LLA), D-lactic acid (DLA) and D,L-lactic acid (DLLA). For the corresponding polymer, PLLA and PDLA are semicrystalline polymers, whereas PDLLA is an amorphous polymer. Since Y. Ikada proposed the stereocomplex (SC) crystallization of PLLA and PDLA in 1987,[12] a large number of studies on the formation of the SC have been reported. On the basis of the triangle shape of SC single crystals and simulation, the growth mechanism was proposed.[13,14] The molecular weight,[15] blending ratio[16] and the architecture[17] of PLLA and PDLA chains show the significant effect on the formation of the SC during the melt−crystallization process.

The most important property of the SC is the melting point (T_m), which is higher than that of neat PLLA by nearly 50 °C.

Received: March 17, 2015
Revised: May 13, 2015
Published: May 27, 2015

DOI: 10.1021/acssuschemeng.5b00214
ACS Sustainable Chem. Eng. 2015, 3, 1492−1500

Investigations on the nucleation effect of the SC on PLLA crystallization behavior have been carried out in the past decades. It has been reported that the SC, as the nucleating agent, can decrease the size of PLLA spherulites.[18,19] It is reported that the nucleation efficiency of the SC can reach approximately 100% when the content of PDLA is 3 wt % with the molecular weight of 14 kg/mol.[20] Although Yang et al.[21] illustrated that the overall crystallization rate was unchanged with PDLA content higher than PDLA percolation concentration (2.0 wt %). However, the SC has little effect on the growth rate of spherulites, though it facilitates the nucleation process.[18] Morphological analysis was also carried out to clarify the relationship between SC crystals and PLLA crystals.[22,23] Unmelted SC crystals can generate cracks in PLLA spherulites during the crystallization process, whereas the cocrystallization of PLLA and the SC is effective in changing the interphases and minimizing the cracks.[23] However, more details related to the morphology evolution from microscopic perspective have not been illustrated.

On the basis of the above analysis, it is worth combining the SC and the flexible PEG chains to manipulate the crystallization behavior of PLA. Kricheldorf et al.[24] studied the crystallization behavior of PLLA-*b*-PEG-*b*-PLLA/PDLA-*b*-PEG-*b*-PDLA with a PLLA or PDLA length of 100 lactic acid units at most, and illustrated that the SC crystals can form independent of the length of soft block. Bao et al.[25] revealed that SC can exclusively form in PLLA (M_w = 21 kg/mol)/PDLA (M_w = 10 kg/mol) blend by adding 10% PEG with molecular weight of 1000 or 2000 g/mol. Rathi et al.[26,27] illustrated that the ductility and flexibility of PLLA was conspicuously improved after blending with PDLA-*b*-PEG-*b*-PDLA or PDLA-*b*-(poly(ethylene−butylene) copolymer) (EB)-*b*-PDLA. Compared with a PLLA/PDLA−poly(ethylene glycol-*co*-propylene glycol) (PEPG)-PDLA blend, the PLLA/PEPG/PDLA blend showed enhanced crystallization of the SC.[28] Liu et al.[29] also reported that the elongation at break increased from 6% to more than 100% when 30 or 40 wt % PDLA-*b*-PEG-*b*-PDLA was added into PLLA; meanwhile, the tensile strengths were maintained.

However, the role of the soft PEG block in the blend, such as the effect on the formation of SC crystals as well as the crystallization and morphology of a PLLA homopolymer, is still not quite clear. In this work, the triblock copolymers PDLA-*b*-PEG-*b*-PDLA with different PEG chain lengths were synthesized. With the blend of PLLA/PDLA as a control, the roles of the PEG block in both the formation of the SC and the subsequent crystallization of the PLLA matrix, and the melting behavior of the blend have been demonstrated. This work is expected to bring a profound understanding of the improved crystallization property of PLLA by blending with the additives combining both the advantages of the SC and flexible PEG chains.

EXPERIMENTAL SECTION

Materials. Poly(L-lactic acid) (PLLA, M_n = 45 000, M_w/M_n = 1.32) and D-lactide (DLA) were purchased from Corbion Purac (The Netherlands). PLLA was purified by precipitating in an excess of cold methanol from dichloromethane solution. DLA was recrystallized from ethyl acetate. PEG (Aldrich, M_n = 400, 1000 and 2000; M_w/M_n = 1.1) was dried with toluene by azeotropic distillation. The molecular weight and distribution of all resultant polymers were determined by ^{1}H NMR (400 MHz, Bruker advance) and gel permeation chromatography (GPC) (waters 2414), respectively.

Synthesis of $PDLA_{2k}$-*b*-PEGx-*b*-$PDLA_{2k}$ and $PDLA_{2k}$. The triblock copolymer was synthesized by ring-opening polymerization of DLA with PEG as a macroinitiator and stannous octoate as a catalyst. The molar ratio of catalyst to the hydroxyl group of PEG was 1:10. The required amounts of DLA monomer, PEG macroinitiator, stannous octoate and toluene were added into a reaction tube under argon atmosphere. By comparison, PDLA was also synthesized under the same conditions except for the ethylene glycol as an initiator. After reaction at 110 °C for 48 h, the copolymers were precipitated in an excess of cold methanol and dried in a vacuum oven. The products are expressed as $PDLA_{2k}$ and $PDLA_{2k}$-*b*-PEG_x-*b*-$PDLA_{2k}$ (x = 0.4k, 1k and 2k), where the subscript represents the molecular weights of PDLA or PEG.

Preparation of PLLA/PDLA-*b*-PEG-*b*-PDLA Blends. Binary blends were obtained by solution-mixing. PLLA and PDLA-*b*-PEG-*b*-PDLA were dissolved in dichloromethane, evaporated in a fume cupboard and dried in a vacuum oven for several days. Two types blends of PLLA/$PDLA_{2k}$ (100/0, 97/3, 95/5, 92/8, 88/12) and PLLA/$PDLA_{2k}$-*b*-PEG_{1k}-*b*-$PDLA_{2k}$ (100/0, 96.25/3.75, 93.75/6.25, 90/10, 85/15) were prepared, which corresponded to the same PDLA segment contents, respectively. For example, PLLA/$PDLA_{2k}$ with 88/12 and PLLA/$PDLA_{2k}$-*b*-PEG_{1k}-*b*-$PDLA_{2k}$ with 85/15 have the same content of PDLA block as 12%.

Characterizations. *Differential Scanning Calorimetry (DSC).* Thermal analysis was performed with DSC (PerkinElmer instrument) under a nitrogen atmosphere at a flow rate of 20 mL/min. For the measurement of T_g, the sample was quenched to 30 °C after erasing the thermal history at 230 °C, and then heated at 20 °C/min. For isothermal crystallization, the blending samples were first heated to 230 °C (190 °C for neat PLLA sample) for 3 min to erase the thermal history and immediately quenched to a given temperature at 100 °C/min and kept there for isothermal crystallization, then heated at 20 °C/min to melting.

Wide Angle X-ray Diffraction (WAXD). The blend samples were melted at 230 °C and compressed at a pressure of 50 kg/cm^2 for 4 min between two Teflon films with a Teflon film of 0.15 mm in thickness as a spacer. Then they were quickly transferred to an oil bath at 150 °C for isothermal crystallization, and finally quenched into ice water. The WAXD data was recorded on a Rigaku D/Max-2500 diffractometer with nickel-filtered Cu Kα radiation (λ = 0.154 nm, 40 kV and 200 mA) in the 2θ range of 5−35° with a scanning rate of 1°/min.

Polarizing Optical Microscopy (POM). A POM (Olympus, BX51) equipped with a Linkham hot stage was used to investigate the crystalline morphology. The blend samples were sandwiched between two glass slides and then melted completely on a hot stage. After the sample was kept at 230 °C (190 °C for neat PLLA sample) for 3 min, it was cooled to a given temperature at 50 °C/min for isothermal crystallization.

Atomic Force Microscopy (AFM). The polymer thin film on silicon wafer was prepared by spin-coating of a droplet of polymer solution (0.4% (w/v)) in chloroform at a speed of 3500 rpm for 40 s. After drying, the thin film was quenched from the melt to a given temperature for isothermal crystallization. The AFM images were obtained at room temperature in ScanAsyst mode with a Nanoscope V MultiMode AFM (digital instruments). Silicon tips with a spring constant of 0.4 N/m were used. The scan rate was 0.977 Hz with a scanning density of 512 lines.

Transmission Electron Microscopy (TEM). The polymer sample was spin-coated on a carbon-coated mica and treated at the same heating history with the samples for AFM. The polymer−carbon thin films were separated from mica by water surface tension and then picked up on a copper grid. The sample was only allowed to dry for electron diffraction purposes. TEM was performed on a JEM-2100 operated at 200 kV.

RESULT AND DISCUSSION

Glass Transition Temperature of Blends. Figure 1 shows the heating scans of different blends after quenched from the melt. The T_g of neat PLLA is 62 °C. For PLLA/PDLA, it decreases to 56 °C with low molecular weight of PDLA acting as a plasticizer. For the blends of PLLA/PDLA-*b*-PEG-*b*-PDLA,

DOI: 10.1021/acssuschemeng.5b00214
ACS Sustainable Chem. Eng. 2015, 3, 1492−1500

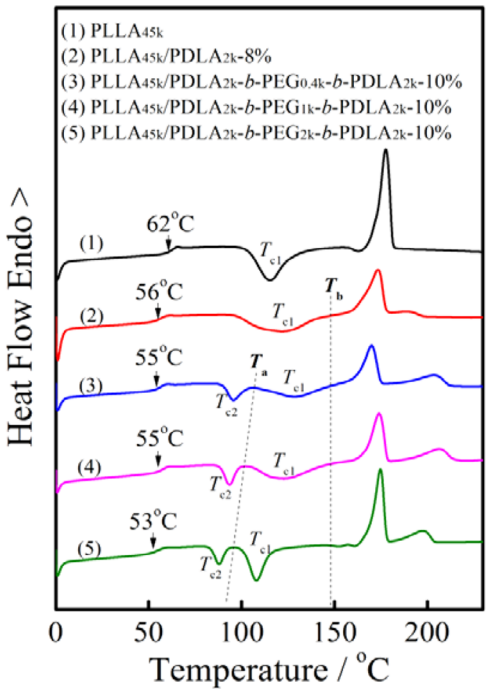

Figure 1. DSC scans of PLLA and its blends after quenched from 230 °C and then heated at a rate of 20 °C/min.

the T_g of the blend with a longer PEG block is lower than that of the blend with a shorter PEG block. These results indicate that both the low molecular weight PDLA and PEG blocks could act as a plasticizer to reduce the T_g of PLLA after blending due to the higher chain mobility of PDLA and the flexibility of PEG chains.

Moreover, upon heating, both neat PLLA and the PLLA/PDLA blend show only one crystallization peak (the peak temperature was marked with T_{c1}), whereas PLLA/PDLA-*b*-PEG-*b*-PDLA blends show two crystallization peaks (the peak temperatures were marked with T_{c1} and T_{c2}). Also, with the increasing length of PEG, these crystallization peaks become sharper and the T_{c2} and T_{c1} shift to lower temperatures. This result illustrates that the longer PEG block is more conducive for improving the crystallization rate of the blends. To illustrate the origin of the two crystallization peaks, the WAXD was conducted on the samples after heating until the temperatures T_a or T_b, at which the two crystallization processes finished, respectively. It should be noted that the second cold crystallization process already started at T_a because of the overlapping of the two peaks for the blend of $PLLA_{45k}$/$PDLA_{2k}$-*b*-$PEG_{0.4k}$-*b*-$PDLA_{2k}$.

As shown in Figure 2a, for the blends of PLLA/PDLA-*b*-PEG-*b*-PDLA after heat treatment to the temperature T_a and then quenched to the room temperature, the diffraction peaks at 11.9°, 20.6° and 23.8° corresponding to the (110), (300)/(030) and (220) of SC crystals[25] are dominate, indicating that the first crystallization peak is resulted from SC formation. The peak at 16.3° assigned to the PLLA crystals in the $PLLA_{45k}$/$PDLA_{2k}$-*b*-$PEG_{0.4k}$-*b*-$PDLA_{2k}$ blend may be resulted from the second crystallization process. For all the blend samples heated to T_b and then quenched to the room temperature, not only the diffraction peaks from the SC crystals but also those at 14.3°, 16.3°, 18.6°, 22.0° corresponding to (010), (110)/(220), (203) and (015) of PLLA crystals[30] are apparently observed, as described in Figure 2b. Therefore, it can be concluded that the formation of the SC is earlier than the crystallization of the PLLA matrix during the heating process in the blends of PLLA/PDLA-*b*-PEG-*b*-PDLA. For the blend of PLLA/PDLA, only little SC crystals accompanied by a majority of PLLA crystals are formed upon heating according to the results of DSC and WAXD.

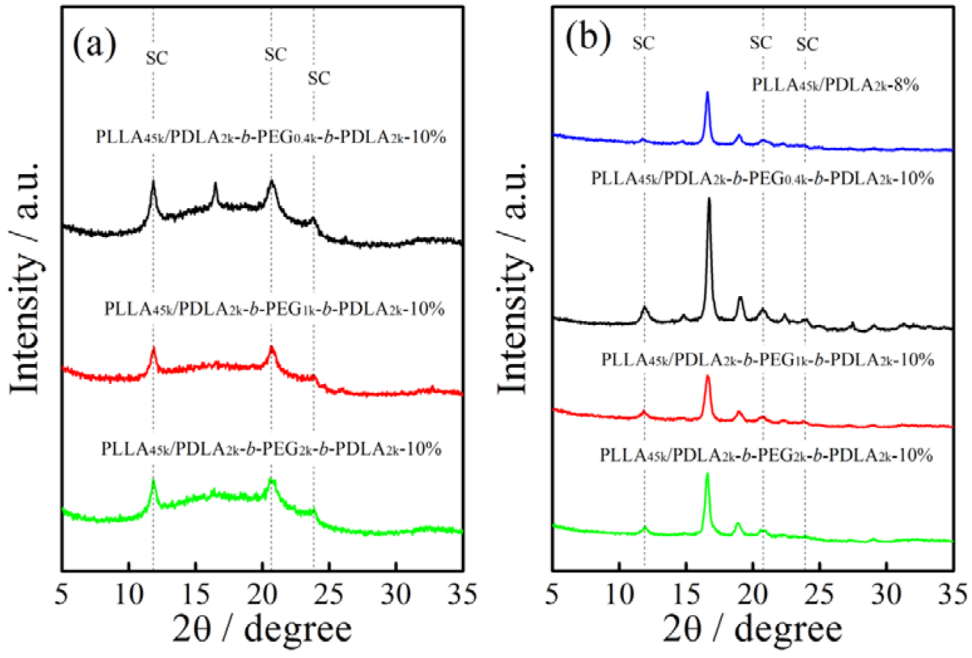

Figure 2. WAXD patterns of PLLA blends with different thermal treatments. (a) Each sample was first quenched from 230 to 0 °C and then heated to its corresponding T_a as indicated in Figure 1. (b) Each sample was first quenched from 230 to 0 °C and then heated to T_b. All WAXD analyses were performed at room temperature.

DOI: 10.1021/acssuschemeng.5b00214
ACS Sustainable Chem. Eng. 2015, 3, 1492−1500

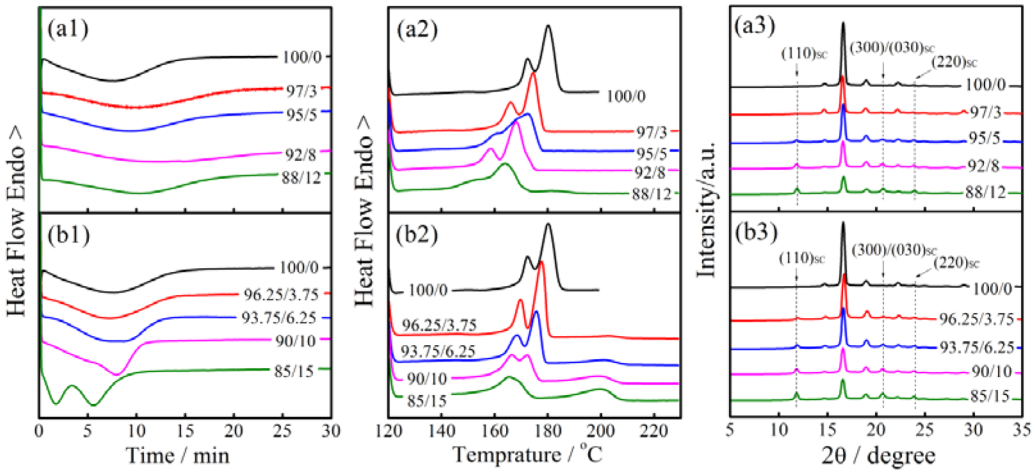

Figure 3. Isothermal crystallization at 120 °C for 1 h and a subsequent heating process at 20 °C/min for PLLA blends. (a1, a2 and a3) Isothermal crystallization, heating process and WAXD patterns of PLLA/$PDLA_{2k}$ with different blending ratios, respectively. (b1, b2 and b3) Those for PLLA/$PDLA_{2k}$-*b*-PEG_{1k}-*b*-$PDLA_{2k}$. The marked three diffraction peaks in WAXD patterns correspond to the SC.

Therefore, as revealed in Figures 1 and 2, the reduction of T_g and apparent earlier formation of the SC in the blends of PLLA/PDLA-*b*-PEG-*b*-PDLA indicate that the PEG chains in the copolymer play an important role in plasticization and stereocomplex crystallization for the blends.

Isothermal Crystallization of the Blends. To tell further the effect of PEG chain on the crystallization of the blend, the $PDLA_{2k}$-*b*-PEG_{1k}-*b*-$PDLA_{2k}$ copolymer with medium molecular weight of PEG was chosen for the following study. Figure 3 shows the DSC curves and WAXD patterns of the blends of PLLA/PDLA and PLLA/PDLA-*b*-PEG-*b*-PDLA with different ratios during and after isothermal crystallization at 120 °C. For the blends of PLLA/PDLA, only one exothermal peak was observed for all the samples, as can be seen in Figure 3a1. Furthermore, this exothermal peak is delayed compared with that of neat PLLA. In the course of heating, the blends show double melting peaks that are lower than those of neat PLLA. Besides, a small lower melting peak appeared at around 183 °C in PLLA/PDLA (88/12), which is higher than the corresponding melting temperature of homocrystals, implying the formation of an imperfect SC during isothermal crystallization at 120 °C. In addition, the WAXD patterns in Figure 3a3 for the blends with the content of PDLA higher than 5% show the diffraction peaks corresponding to the SC crystals, confirming the formation of the SC. The deviation between the two techniques may be due to the different sensitivities. These results indicate that the PDLA, which plays the role of plasticizer for PLLA after blending, reduces both the crystallization rate and melting temperature of the PLLA/PDLA blend.

For PLLA/PDLA-*b*-PEG-*b*-PDLA blends, the isothermal crystallization curves are very different from those of PLLA/PDLA blends. As presented in Figure 3b1, two apparent exothermal peaks emerge for the blends with the amount of copolymer more than 6.25% in the blends, and the crystallization time is shorter than that of neat PLLA. For the corresponding melting curves in Figure 3b2, one melting peak around 200 °C appears besides the double melting peaks around 170 °C, and it becomes stronger with more copolymer in the blends, suggesting the formation of the SC. This is corroborated by the WAXD patterns in Figure 3b3, which shows clear diffraction peaks at 11.9°, 20.6° and 23.8°. Besides, two melting peaks are observed at 165−180 °C for the blend of PLLA/PDLA-*b*-PEG-*b*-PDLA. The DSC heating scans with different heating rates after crystallization at 120 °C for 30 min confirm that the two melting peaks are caused by original and melt-recrystallized PLLA crystals (see Figure S1 of the Supporting Information).

Therefore, on the basis of the results in Figure 3, it is concluded that both the PDLA homopolymer and PDLA-*b*-PEG-*b*-PDLA copolymer could result in the formation of the SC after blending with PLLA. Moreover, the PEG block chains not only contribute to the easier formation of SC in the blends but also promote the crystallization of PLLA in the blends.

To reveal further the origin of the two exothermal peaks in Figure 3b1 for the blends of PLLA/PDLA-*b*-PEG-*b*-PDLA, the immediate heating process after isothermal crystallization at 120 °C for different times was investigated, and the results are shown in Figure 4 and Table S2 of the Supporting Information.

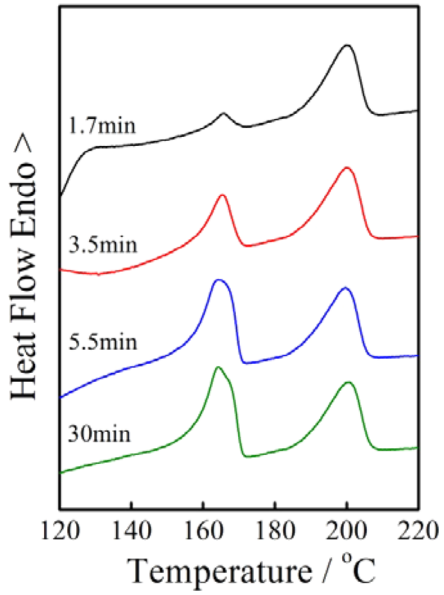

Figure 4. DSC heating curves of PLLA/$PDLA_{2k}$-*b*-PEG_{1k}-*b*-$PDLA_{2k}$ (85/15) at a rate of 20 °C/min after isothermal crystallization at 120 °C for different times.

DOI: 10.1021/acssuschemeng.5b00214
ACS Sustainable Chem. Eng. 2015, 3, 1492−1500

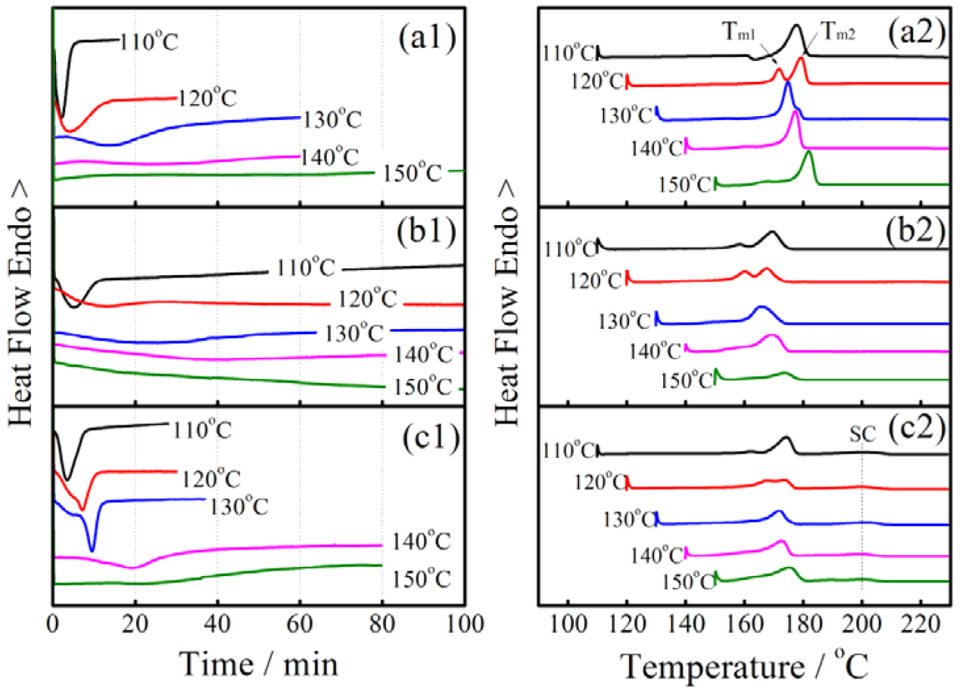

Figure 5. DSC curves of isothermal crystallization process (a1, b1, c1) at different temperatures and subsequently heating processes (a2, b2, c2). (a1, a2) Neat PLLA. (b1, b2) PLLA/$PDLA_{2k}$ (92/8). (c1, c2) PLLA/$PDLA_{2k}$-*b*-PEG_{1k}-*b*-$PDLA_{2k}$ (90/10).

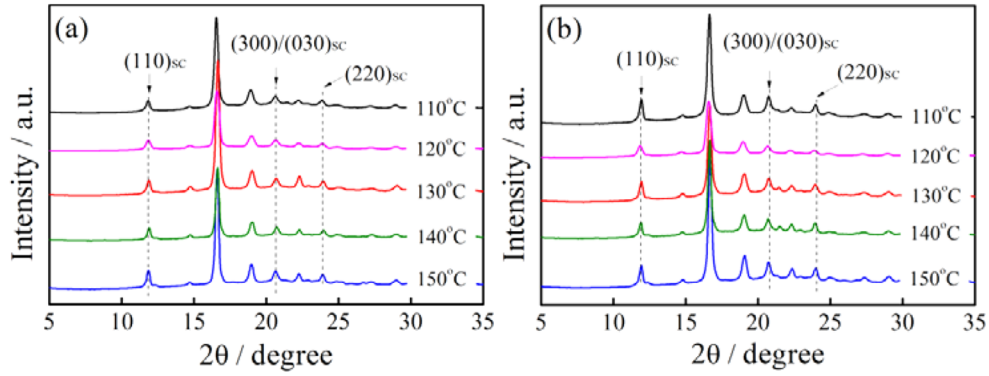

Figure 6. WAXD patterns of PLLA blends after isothermal crystallization at different temperatures for 2 h. (a) PLLA/$PDLA_{2k}$ (92/8). (b) PLLA/$PDLA_{2k}$-*b*-PEG_{1k}-*b*-$PDLA_{2k}$ (90/10).

After crystallization at 120 °C for only 1.7 min, the melting peak at 210 °C corresponding to the SC becomes very clear and almost reaches the maximum enthalpy (ΔH = 19.8 J/g), whereas the melting peak at 170 °C just begins to crop up. Further extending crystallization time, the two melting peaks become clearer and the relative intensity is almost unchanged eventually. The results in Figure 4 indicate that the SC forms first and then the PLLA starts to crystallize in the course of isothermal crystallization for PLLA/PDLA-*b*-PEG-*b*-PDLA blends. Compared to the melting behavior of PLLA/PDLA, it could be concluded that it is the PEG block that plays an important role in promoting SC formation for PDLA/PDLA-*b*-PEG-*b*-PDLA blends.

Figure 5 shows the isothermal crystallization at different temperatures and the corresponding melting behaviors for PLLA, PLLA/PDLA and PLLA/PDLA-*b*-PEG-*b*-PDLA. For PLLA, the isothermal crystallization curve at a given temperature shows only one exothermic peak (Figure 5a1). The shift of this peak toward longer time region indicates the slower crystallization rate at higher temperatures. The melting curve of PLLA at 120 °C in Figure 5a2 shows double melting peaks (T_{m1} and T_{m2}) that arise from original crystals during the crystallization process and recrystallization of imperfect crystals upon heating, respectively. The changes of position and relative areas of double melting peaks with crystallization temperatures reflect the perfectness and recrystallizability of PLLA after isothermal crystallization at different temperatures.

For the blends of PLLA/PDLA, as shown in Figure 5b1,2, both the crystallization and melting behaviors show similarities with those of neat PLLA. The only difference is that the crystallization peak of PLLA/PDLA blends is postponed compared with that of neat PLLA. The main reason is that the 8% PDLA with a lower molecular weight may play the diluting role for the PLLA matrix, resulting in the slower crystallization rate of PLLA in blends.

For the blends of PLLA/PDLA-*b*-PEG-*b*-PDLA, as shown in Figure 5c1,2, at higher crystallization temperatures (e.g., T_c > 120 °C), the crystallization curves show obvious exothermic peak(s) at shorter time regions compared to that of the PLLA or PLLA/PDLA blend. The reciprocal of the peak time ($1/t_p$)

DOI: 10.1021/acssuschemeng.5b00214
ACS Sustainable Chem. Eng. 2015, 3, 1492−1500

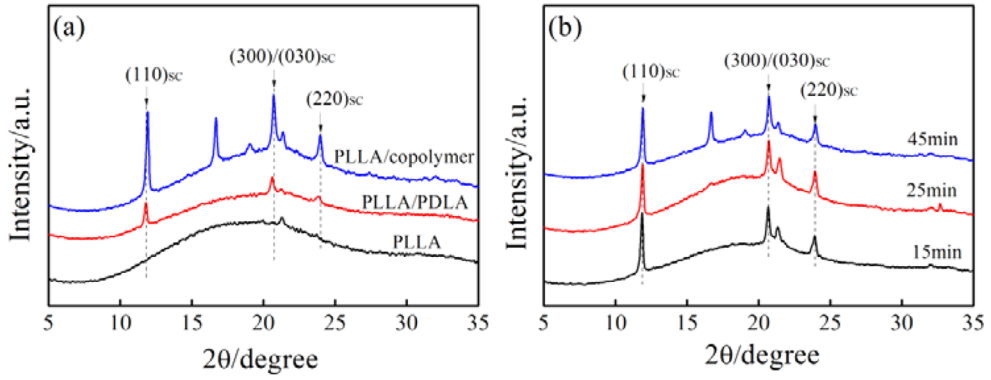

Figure 7. (a) WAXD patterns of neat PLLA, PLLA/PDLA$_{2k}$ (92/8) and PLLA/PDLA$_{2k}$-*b*-PEG$_{1k}$-*b*-PDLA$_{2k}$ (90/10) after isothermal crystallization at 150 °C for 45 min. (b) WAXD patterns of PLLA/PDLA$_{2k}$-*b*-PEG$_{1k}$-*b*-PDLA$_{2k}$ (90/10) after isothermal crystallization at 150 °C for 15, 25 and 45 min, respectively.

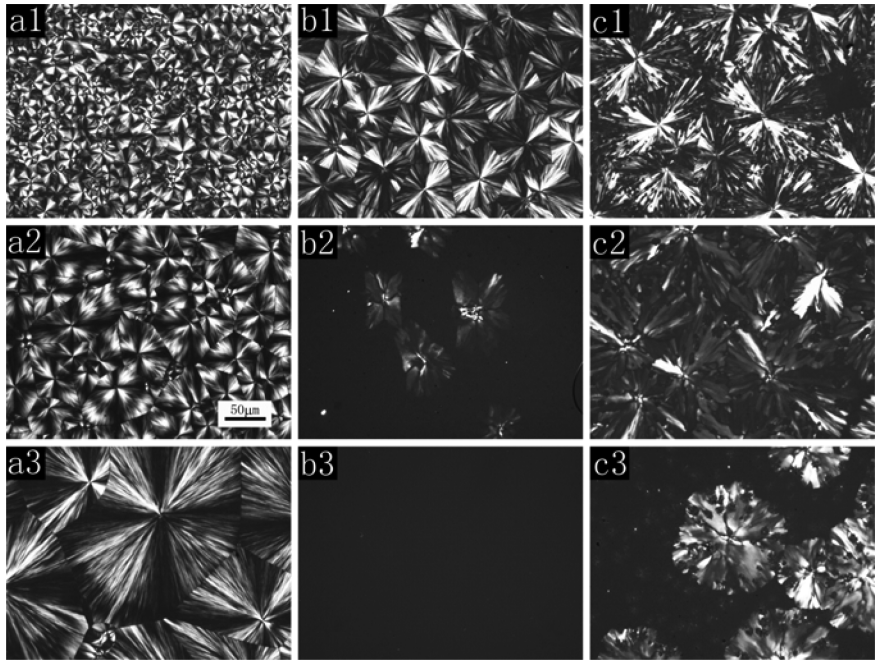

Figure 8. Polarized optical micrographs of PLLA, PLLA/PDLA (92/8) and PLLA/PDLA$_{2k}$-*b*-PEG$_{1k}$-*b*-PDLA$_{2k}$ (90/10) blends after isothermal crystallization. (a1) PLLA, 110 °C, 15 min. (b1) PLLA/PDLA, 110 °C, 33 min. (c1) PLLA/PDLA$_{2k}$-*b*-PEG$_{1k}$-*b*-PDLA$_{2k}$, 110 °C, 32 min. (a2) PLLA, 120 °C, 20 min. (b2) PLLA/PDLA, 120 °C, 90 min. (c2) PLLA/PDLA$_{2k}$-*b*-PEG$_{1k}$-*b*-PDLA$_{2k}$, 120 °C, 90 min. (a3) PLLA, 130 °C, 90 min. (b3) PLLA/PDLA, 130 °C, 90 min. (c3) PLLA/PDLA$_{2k}$-*b*-PEG$_{1k}$-*b*-PDLA$_{2k}$, 130 °C, 49 min.

of PLLA/PDLA is the lowest at all crystallization temperatures. The $1/t_p$ of PLLA/PDLA-*b*-PEG-*b*-PDLA exceeds neat PLLA at T_c > 120 °C, which means that the crystallization rate of the PLLA/PDLA-*b*-PEG-*b*-PDLA blend is the highest at higher crystallization temperatures (see Figure S2 of the Supporting Information). Moreover, in addition to the melting peaks from PLLA around 170 °C, an endothermic peak around 200 °C arising from the SC is clearly seen for the blends of PLLA/PDLA-*b*-PEG-*b*-PDLA after melt−crystallization. Therefore, it could be concluded that the faster crystallization rate at higher temperatures for the blends of PLLA/PDLA-*b*-PEG-*b*-PDLA is due to the nucleation function of the SC, compared to the PLLA or the PLLA/PDLA blend.

Figure 6 shows the WAXD patterns of the PLLA/PDLA and PLLA/PDLA-*b*-PEG-*b*-PDLA blends after isothermal crystallization at different temperatures. In addition to the diffraction peaks from PLLA crystals, the peaks corresponding to SC crystals are also apparently observed. These results indicate that not only the PLLA/PDLA-*b*-PEG-*b*-PDLA blend but also the PLLA/PDLA blend could form the SC, even though the melting peak of the SC could not be observed in Figure 5b2 for the blend of PLLA/PDLA. Therefore, it can be summarized from Figures 5 and 6 that the influences of the PDLA homopolymer and PDLA-*b*-PEG-*b*-PDLA copolymer on the crystallization and melting behavior of their PLLA blends are different.

Compared with PDLA, PDLA-*b*-PEG-*b*-PDLA shows a better promotion role in the formation of the SC and the crystallization of the PLLA matrix after blending, which should attribute to the PEG block. For the blends of PLLA/PDLA-*b*-PEG-*b*-PDLA when isothermal crystallized at temperatures above 70 °C, the PEG block chains were in the melting state. These PEG chains are flexible and compatible with the PLLA matrix to form a continuous amorphous phase.[27] Therefore, when the blends crystallize isothermally, the flexible PEG chains which act as diluting agent or solvent can greatly

DOI: 10.1021/acssuschemeng.5b00214
ACS Sustainable Chem. Eng. 2015, 3, 1492−1500

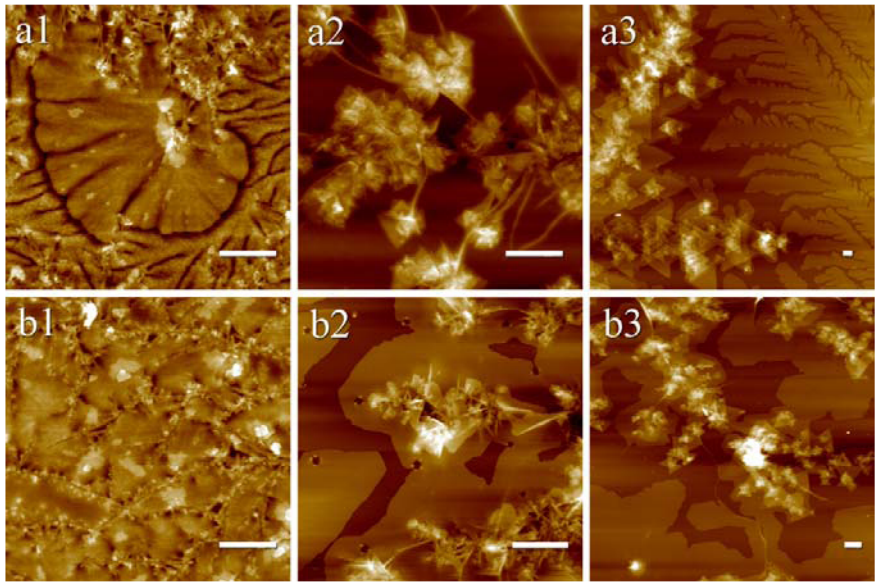

Figure 9. AFM images of PLLA/PDLA$_{2k}$ (92/8) (a1−a3) and PLLA/PDLA$_{2k}$-*b*-PEG$_{1k}$-*b*-PDLA$_{2k}$ (90/10) (b1−b3) after isothermal crystallization. (a1, b1) 110 °C, 1.5 h, (a2, b2) 130 °C, 4 h, (a3, b3) 150 °C, 40 h. The scale bar is 1 μm.

facilitate the motion of PDLA block chains of the copolymer and the PLLA chains of the matrix. As a result, the SC in the blend of PLLA/PDLA-*b*-PEG-*b*-PDLA is encouraged to form, and in turn can act as a nucleating agent for the crystallization of the PLLA matrix.

To elucidate further the promoting role of PEG in the formation of the SC, the dependence of SC crystals and PLLA crystals on the crystallization time was studied, and the results are shown in Figure 7. After crystallization at 150 °C for 45 min, PLLA is still in the amorphous state without any characteristic diffraction peaks, whereas the blends of PLLA/PDLA reveal the diffraction peaks at 11.9°, 20.6° and 23.8°, indicating the formation of only SC crystals. Interestingly, the blends of PLLA/PDLA-*b*-PEG-*b*-PDLA show sharp diffraction peaks corresponding to both SC crystals and PLLA crystals. The results in Figure 7a indicate that it is the PEG chains in the blends of PLLA/PDLA-*b*-PEG-*b*-PDLA that promote the formation of both SC crystals and PLLA crystals. It is further found from Figure 7b that the first appearance of diffraction peaks are from SC crystals, and then the diffraction peaks from PLLA crystals are seen after crystallization for 45 min. The sequent formation of the SC crystal and PLLA crystal in Figure 7 clearly demonstrates that the PEG chains in the blend of PLLA/copolymer first promote the formation of the SC, whereas the formed SC may act as nucleating agents at higher crystallization temperatures to induce the crystallization of the PLLA matrix. These conclusions are also in accordance with the DSC and WAXD results in Figures 1 and 2.

Crystalline Morphology of Blends. Figure 8 shows the typical polarized optical micrographs of neat PLLA, the blends of PLLA/PDLA and PLLA/PDLA-*b*-PEG-*b*-PDLA after isothermal crystallization at 110, 120 and 130 °C, respectively. For neat PLLA, spherulites with small size (Figure 8a1) were formed at 110 °C due to the large supercooling degree and fast nucleation rate. The size of spherulites increases with crystallization temperature due to the difficulty of nucleation, as shown in Figure 8a2,3.

For the blends of PLLA/PDLA, the size of spherulites is obviously larger compared with that of neat PLLA at 110 °C (Figure 8b1). With increasing crystallization temperature, the crystallization becomes more difficult and the spherulites are hard to observe at 130 °C after crystallization for 90 min. The low crystallization rate of PLLA/PDLA blends is in accordance with the DSC results, as illustrated in Figure 8 and Figure S2 of the Supporting Information. The dilution effect of PDLA with a low molecular weight of 2000 g/mol is the main factor resulting in the reduction of the nucleation ability of the PLLA matrix.

For the blends of PLLA/PDLA-*b*-PEG-*b*-PDLA, the size of spherulites increases slightly when the crystallization temperature increases from 110 to 130 °C. Compared to the neat PLLA, the size of spherulites of PLLA/PDLA-*b*-PEG-*b*-PDLA is larger at 110 °C (Figure 8c1), but smaller at 130 °C (Figure 8c3). The results in Figure 6b show that SC crystals are formed in the range of temperatures from 110 to 150 °C. It has been reported that the preformed SC crystallite network may confine the crystallization of the PLLA matrix due to the restriction of PLLA chains.[21,30] Therefore, for the blends of PLLA/PDLA-*b*-PEG-*b*-PDLA, when crystallized at lower temperatures (e.g., 110 °C), the soft PEG block enhances the SC formation, as the numerous bright "dots" shown in Figure 8c1, whereas on the other hand, the dilution effect by residual PEG chains and the confinement effect by SC nuclei might result in the decrease of nucleation density. At higher temperatures (e.g., 130 °C), when the nucleation is the control step, the SC crystallites are also formed first, and then the nucleation effect of preformed SC crystals facilitate the nucleation of the PLLA matrix.

The results in Figure 8 demonstrate the complex roles of plasticization and SC in the crystallization for the blends of PLLA/copolymer. Our results indicate that the PEG block chains facilitate the formation of SC for the blends of PLLA/PDLA-*b*-PEG-*b*-PDLA. However, as reported by Sahas Rathi et al.,[28] the connected PEPG block in PLLA/PDLA-*b*-PEPG-*b*-PDLA can make the SC crystallize slower compared with PLLA/PEPG/PDLA. Therefore, further investigation on the effects of covalently linked PEG block from block copolymers or individual PEG chains in the blends on the SC formation and PLLA crystallization is still needed in the future.

DOI: 10.1021/acssuschemeng.5b00214
ACS Sustainable Chem. Eng. 2015, 3, 1492−1500

From the viewpoint of spherulite morphology, the neat PLLA and PLLA/PDLA blends show typical spherulites with a clear maltese cross, whereas the blend of PLLA/copolymer at higher crystallization temperatures shows dendrites without a maltese cross. To reveal further the morphological structures, the thin films of PLLA blends after isothermal crystallization at different temperatures were examined by AFM and the results are shown in Figure 9.

As can be seen in Figure 9, the blends of PLLA/PDLA and PLLA/PDLA-*b*-PEG-*b*-PDLA show different lamellar morphologies at different crystallization temperatures. At 110 °C, the blend of PLLA/PDLA presents spherulites with a small amount of randomly distributed string-like crystals on the surface (Figure 9a1), whereas the blend of PLLA/PDLA-*b*-PEG-*b*-PDLA shows flat-on lamellae with a large amount of string-like crystals (Figure 9b1). When the crystallization temperature increases to 130 °C, the blend of PLLA/PDLA exhibits only the dense string-like crystals and disordered stacking lamellae (Figure 9a2), whereas the blend of PLLA/copolymer displays not only the string-like crystals and disordered stacking lamellae but also the large single-deck flat-on lamellae (Figure 9b2). At 150 °C, the string-like crystals and disordered stacking lamellae become regularly stacked lamellae with triangular shape in the blends of PLLA/PDLA. In addition, large single-layered lamellae, besides the triangular crystals, are also observed. For the blend of PLLA/copolymer, only the flat-on lamellar crystals below the string-like crystals and disordered stacking lamellae are mainly detected, similar to that at 130 °C (Figure 9b2,3). Yet, the triangular crystals for PLLA/copolymer at 150 °C can still be identified, as shown in Figure 9b3.

The lamellar crystal structure with different morphologies was verified by the further analysis of electron diffraction. In Figure 10, the diffraction patterns at the top right and lower right corners are corresponding to SC and PLLA crystals, respectively,[14,31] which means the triangular crystals and the large single-deck lamellae are SC and PLLA crystals, correspondingly.

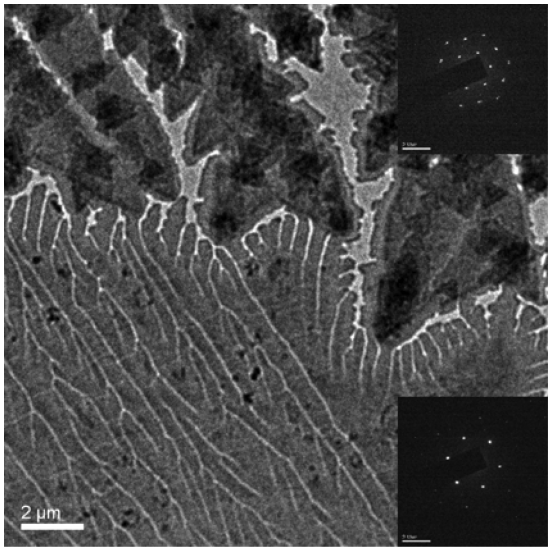

Figure 10. Transmission electron micrograph of the PLLA/PDLA blend after crystallization at 150 °C for 40 h on the silica coated with carbon. Electron diffraction patterns of the crystal inserted in the top and bottom right corners.

Therefore, the AFM results at the lamellar level clearly reveal the morphological differences in string-like crystals and flat-on crystals for the blends of PLLA/PDLA and PLLA/copolymer, which reflects the different growth behaviors of the SC and the PLLA matrix. For the blends of PLLA/copolymer, not only are the SC crystals more easily formed but also the PLLA flat-on lamellae can be formed compared to the blends of PLLA/PDLA. The morphological results from both spherulite and lamellar levels indicate again that the flexible PEG block plays an important role in the promotion of crystallization for both the SC and the PLLA matrix.

CONCLUSIONS

The isothermal crystallization behavior and corresponding morphology evolution of neat PLLA and its blends with PDLA or PDLA-*b*-PEG-*b*-PDLA were investigated by DSC, WAXD, POM, AFM and TEM. The gradual reduction of T_g and cold crystallization temperature of the SC for the blends with longer PEG chains implies the important role of PEG chains in the crystallization of PLLA/PDLA-*b*-PEG-*b*-PDLA blends. Compared to the PLLA/PDLA blend, the PLLA/PDLA-*b*-PEG-*b*-PDLA blend shows easier formation of the SC and a faster crystallization rate of the PLLA matrix. DSC and WAXD results corroborate that the SC is first formed and subsequently accelerates the crystallization of the PLLA matrix for the blends. In consideration of the miscible nature and the low melting point of PEG, the melted PEG chains of copolymer act as diluting agents to promote the formation of the SC by facilitating the motion of PDLA chains of copolymer and PLLA chains of the matrix during crystallization process for PLLA/PDLA-*b*-PEG-*b*-PDLA blends. This work indicates that the flexible PEG block chains play a significant role in the promotion of crystallization for both the SC and the PLLA matrix.

ASSOCIATED CONTENT

Supporting Information

Thermal characteristics of DSC isothermal and heating scans for the specific specimens, multiple melting behavior of PLLA/PDLA-*b*-PEG-*b*-PDLA, and the crystallization rates of PLLA, PLLA/PDLA and PLLA/PDLA-*b*-PEG-*b*-PDLA. The Supporting Information is available free of charge on the ACS Publications website at DOI: 10.1021/acssuschemeng.5b00214.

AUTHOR INFORMATION

Corresponding Authors

*Z.G. Tel./fax: +86-10-64432762. E-mail: zhgan@mail.buct.edu.cn.

*N.J. Tel./fax: +86-10-64432762. E-mail: jiangni@iccas.ac.cn.

Notes

The authors declare no competing financial interest.

ACKNOWLEDGMENTS

This work was supported by the National Natural Science Foundation of China (Grant no. 51025314, 21104089).

REFERENCES

(1) Auras, R.; Harte, B.; Selke, S. An overview of polylactides as packaging materials. *Macromol. Biosci.* **2004**, *4* (9), 835−864.

(2) Xu, H.; Xie, L.; Chen, Y.-H.; Huang, H.-D.; Xu, J.-Z.; Zhong, G.-J.; Hsiao, B. S.; Li, Z.-M. Strong shear flow-driven simultaneous formation of classic shish-kebab, hybrid shish-kebab, and trans-

DOI: 10.1021/acssuschemeng.5b00214
ACS Sustainable Chem. Eng. 2015, 3, 1492−1500

crystallinity in poly(lactic acid)/natural fiber biocomposites. *ACS Sustainable Chem. Eng.* **2013**, *1* (12), 1619−1629.
(3) Zhong, Y.; Fang, H.; Zhang, Y.; Wang, Z.; Yang, J.; Wang, Z. Rheologically determined critical shear rates for shear-induced nucleation rate enhancements of poly(lactic acid). *ACS Sustainable Chem. Eng.* **2013**, *1* (6), 663−672.
(4) Desai, N. P.; Hubbell, J. A. Solution technique to incorporate polyethylene oxide and other water-soluble polymers into surfaces of polymeric biomaterials. *Biomaterials* **1991**, *12* (2), 144−153.
(5) Sheth, M.; Kumar, R. A.; Davé, V.; Gross, R. A.; McCarthy, S. P. Biodegradable polymer blends of poly(lactic acid) and poly(ethylene glycol). *J. Appl. Polym. Sci.* **1997**, *66* (8), 1495−1505.
(6) Baiardo, M.; Frisoni, G.; Scandola, M.; Rimelen, M.; Lips, D.; Ruffieux, K.; Wintermantel, E. Thermal and mechanical properties of plasticized poly(L-lactic acid). *J. Appl. Polym. Sci.* **2003**, *90* (7), 1731−1738.
(7) Nijenhuis, A. J.; Colstee, E.; Grijpma, D. W.; Pennings, A. J. High molecular weight poly(L-lactide) and poly(ethylene oxide) blends: Thermal characterization and physical properties. *Polymer* **1996**, *37* (26), 5849−5857.
(8) Younes, H.; Cohn, D. Phase-separation in poly(ethylene glycol) poly(lactic acid) blends. *Eur. Polym. J.* **1988**, *24* (8), 765−773.
(9) Lai, W. C.; Liau, W. B.; Lin, T. T. The effect of end groups of PEG on the crystallization behaviors of binary crystalline polymer blends PEG/PLLA. *Polymer* **2004**, *45* (9), 3073−3080.
(10) Hu, Y.; Hu, Y. S.; Topolkaraev, V.; Hiltner, A.; Baer, E. Crystallization and phase separation in blends of high stereoregular poly(lactide) with poly(ethylene glycol). *Polymer* **2003**, *44* (19), 5681−5689.
(11) Hu, Y.; Hu, Y. S.; Topolkaraev, V.; Hiltner, A.; Baer, E. Aging of poly(lactide)/poly(ethylene glycol) blends. Part 2. Poly(lactide) with high stereoregularity. *Polymer* **2003**, *44* (19), 5711−5720.
(12) Ikada, Y.; Jamshidi, K.; Tsuji, H.; Hyon, S. H. Stereocomplex formation between enantiomeric poly(lactides). *Macromolecules* **1987**, *20* (4), 904−906.
(13) Brizzolara, D.; Cantow, H. J.; Diederichs, K.; Keller, E.; Domb, A. J. Mechanism of the stereocomplex formation between enantiomeric poly(lactide)s. *Macromolecules* **1996**, *29* (1), 191−197.
(14) Cartier, L.; Okihara, T.; Lotz, B. Triangular polymer single crystals: Stereocomplexes, twins, and frustrated structures. *Macromolecules* **1997**, *30* (20), 6313−6322.
(15) Tsuji, H.; Ikada, Y. Stereocomplex formation between enantiomeric poly(lactic acid)s .9. Stereocomplexation from the melt. *Macromolecules* **1993**, *26* (25), 6918−6926.
(16) Brochu, S.; Prudhomme, R. E.; Barakat, I.; Jerome, R. Stereocomplexation and morphology of polylactides. *Macromolecules* **1995**, *28* (15), 5230−5239.
(17) Shao, J.; Tang, Z.; Sun, J.; Li, G.; Chen, X. Linear and four-armed poly(L-lactide)-block-poly(D-lactide) copolymers and their stereocomplexation with poly(lactide)s. *J. Polym. Sci. Polym. Phys.* **2014**, *52* (23), 1560−1567.
(18) Rahman, N.; Kawai, T.; Matsuba, G.; Nishida, K.; Kanaya, T.; Watanabe, H.; Okamoto, H.; Kato, M.; Usuki, A.; Matsuda, M.; Nakajima, K.; Honma, N. Effect of polylactide stereocomplex on the crystallization behavior of poly(L-lactic acid). *Macromolecules* **2009**, *42* (13), 4739−4745.
(19) Schmidt, S. C.; Hillmyer, M. A. Polylactide stereocomplex crystallites as nucleating agents for isotactic polylactide. *J. Polym. Sci. Polym. Phys.* **2001**, *39* (3), 300−313.
(20) Wei, X. F.; Bao, R. Y.; Cao, Z. Q.; Yang, W.; Xie, B. H.; Yang, M. B. Stereocomplex crystallite network in asymmetric PLLA/PDLA blends: Formation, structure, and confining effect on the crystallization rate of homocrystallites. *Macromolecules* **2014**, *47* (4), 1439−1448.
(21) Anderson, K. S.; Hillmyer, M. A. Melt preparation and nucleation efficiency of polylactide stereocomplex crystallites. *Polymer* **2006**, *47* (6), 2030−2035.
(22) Woo, E. M.; Chang, L. Crystallization and morphology of stereocomplexes in nonequimolar mixtures of poly(L-lactic acid) with excess poly(D-lactic acid). *Polymer* **2011**, *52* (26), 6080−6089.
(23) Nurkhamidah, S.; Woo, E. M. Effects of stereocomplex nuclei or spherulites on crystalline morphology and crack behavior of poly(L-lactic acid). *Macromol. Chem. Phys.* **2011**, *212* (15), 1663−1670.
(24) Kricheldorf, H. R.; Rost, S.; Wutz, C.; Domb, A. Stereocomplexes of A-B-A triblock copolymers based on poly(L-lactide) and poly(D-lactide) A blocks. *Macromolecules* **2005**, *38* (16), 7018−7025.
(25) Bao, R. Y.; Yang, W.; Wei, X. F.; Xie, B. H.; Yang, M. B. Enhanced formation of stereocomplex crystallites of high molecular weight poly(L-lactide)/poly(D-lactide) blends from melt by using poly(ethylene glycol). *ACS Sustainable Chem. Eng.* **2014**, *2* (10), 2301−2309.
(26) Rathi, S.; Chen, X.; Coughlin, E. B.; Hsu, S. L.; Golub, C. S.; Tzivanis, M. J. Toughening semicrystalline poly(lactic acid) by morphology alteration. *Polymer* **2011**, *52* (19), 4184−4188.
(27) Rathi, S. R.; Coughlin, E. B.; Hsu, S. L.; Golub, C. S.; Ling, G. H.; Tzivanis, M. J. Effect of midblock on the morphology and properties of blends of ABA triblock copolymers of PDLA-mid-block-PDLA with PLLA. *Polymer* **2012**, *53* (14), 3008−3016.
(28) Rathi, S. R.; Ng, D.; Coughlin, E. B.; Hsu, S. L.; Golub, C. S.; Ling, G. H.; Tzivanis, M. J. Effects of molecular architecture on the stereocomplex crystallization in poly(lactic acid) blends. *Macromol. Chem. Phys.* **2014**, *215* (4), 320−326.
(29) Liu, Y.; Shao, J.; Sun, J.; Bian, X.; Feng, L.; Xiang, S.; Sun, B.; Chen, Z.; Li, G.; Chen, X. Improved mechanical and thermal properties of PLLA by solvent blending with PDLA-b-PEG-b-PDLA. *Polym. Degrad. Stab.* **2014**, *101* (0), 10−17.
(30) Shao, J.; Sun, J.; Bian, X.; Cui, Y.; Zhou, Y.; Li, G.; Chen, X. Modified PLA homochiral crystallites facilitated by the confinement of PLA stereocomplexes. *Macromolecules* **2013**, *46* (17), 6963−6971.
(31) Aleman, C.; Lotz, B.; Puiggali, J. Crystal structure of the alpha-form of poly(L-lactide). *Macromolecules* **2001**, *34* (14), 4795−4801.

DOI: 10.1021/acssuschemeng.5b00214
ACS Sustainable Chem. Eng. 2015, 3, 1492−1500